

Impact of Land Surface Processes on Boundary Layer Evolution

William T. Thompson and Teddy Holt
Naval Research Laboratory
Monterey, CA

Hao Jin
SAIC
Monterey, CA

1, INTRODUCTION

The effect of land-vegetative processes and the corresponding dynamical impact on land-atmosphere interactions is investigated in the context of the International H₂O Project (IHOP_2002) field experiment (Weckwerth et al. 2004). The primary motivation for this work is to evaluate surface properties from the land surface model (LSM) and to investigate the impact of the LSM on boundary layer structure. Land-vegetative processes, as driven by features such as surface heterogeneity (Pielke 2001) or soil moisture gradients (Chang and Wetzel 1991) have been shown to be important mechanisms in the development of convection. Chang and Wetzel (1991) show that vegetation gradients can also be important influences on boundary layer structure. Strong gradients in surface fluxes resulting from these in homogeneities can drive mesoscale circulations.

The objective of this study is to investigate the sensitivity of the parameterization of land-vegetative processes in a nonhydrostatic mesoscale model.

2. MODEL DESCRIPTION

The atmospheric component of the Naval Research Laboratory's (NRL) Coupled Ocean/Atmosphere Mesoscale Prediction

Corresponding Author: William T. Thompson, Naval Research Laboratory, Monterey, CA 93943, william.thompson@nrlmry.navy.mil

System (COAMPS *) with non-hydrostatic dynamics is used for the numerical model simulations. For this study COAMPS is configured with three one-way interactive nests of 36 km and 12 km over the central US and 4 km centered over the IHOP_2002 observation region (Fig. 1). The emphasis is on the higher resolution 4-km nest, so all subsequent figures and discussion will pertain to nest 3. In the vertical, 60 levels are used from the surface to ~25.5 Km with 13 grid points in the lowest 100 m and 29 levels below 1 km. The spacing stretches to several km at higher elevations.

Model physical parameterization schemes include the Weather Research and Forecasting (WRF) Noah Land Surface Model (LSM) and the WRF canopy resistance formulation, The WRF Noah land-surface/hydrology model (Pan and Mahrt 1987) is based on the coupling of the diurnally-dependent Penman potential evaporation approach of Mahrt and Ek (1984), the multi-layer soil model of Mahrt and Pan (1984), and the one-layer canopy model of Pan and Mahrt (1987). The canopy resistance formulation has been extended by Chen et al. (1996) to include the modestly complex Jarvis-type canopy resistance parameterization. Global observation-based analyses at 45 km resolution are used to drive the WRF Noah LSM.

The mesoscale variability of vegetation and soil characteristics in the region is from

*COAMPS is a registered trademark of the Naval Research Laboratory

the United States Geological Survey (USGS) 24-category 30-second dataset and the soil texture derived from the U.S. Department of Agriculture 16-category State Soil Geographic Database (STATSGO). This formulation allows moisture to be released to the atmosphere via transpiration, which is one of the most efficient means of water loss from the vegetated land surface. The canopy resistance of the WRF Noah scheme is a function of minimal stomatal resistance (vegetation type-based), leaf area index and effects of solar radiation, water stress, vapor pressure deficit, and air temperature as defined in Noilhan and Planton (1989).

For the first simulation only (0000 UTC 01 June), initial conditions (i.e., model first guess fields) are obtained by interpolating from the 1-degree fields from the Navy Operational Global Atmosphere Prediction System (NOGAPS) to the COAMPS domain. Subsequent first guess fields for all other simulations use the previous COAMPS 12 h forecast. Boundary conditions for all simulations are derived from 6-hourly NOGAPS forecasts,

3. RESULTS

Twice-daily 24 h COAMPS forecasts with the LSM were produced for the first 12 days of June 2002. Control forecast without the LSM were produced for selected periods (in the absence of the LSM, COAMPS uses a simple slab soil model with no vegetative canopy). For each forecast beginning at 0000 UTC, time series of 24 h duration were produced showing the model forecast and the observations for each of eight Integrated Surface Flux Facility (ISFF) stations operated during IHOP-2002. Time series were produced for surface temperature, 2 m air temperature, 2 m mixing ratio, 2 m wind speed and direction, surface sensible heat flux, surface latent heat flux, ground surface heat flux, surface stress, long wave radiative flux, short wave flux, and net radiation. Shown in Fig. 2a and b are surface temperature and 2 m air temperature ($^{\circ}\text{C}$) for ISFF station 4 (37.36°N , 98.24°W) valid 0000 UTC 6 June-0000UTC (1900 LT) 7 June 2002 for the LSM (Fig 2a) and the control (Fig 2b). Note that the LSM more nearly

captures not only the value of the surface and 2 m temperature but also the temporal variation, particularly near dawn. This improvement in the diurnal cycle is characteristic of many cases. The surface sensible and latent heat fluxes are shown in Fig 3. The sensible heat flux in the LSM (Fig 3a) is somewhat closer to the observed flux (control is too large) while the latent heat flux (Fig 3b) is substantially improved in the LSM (control is too low). The latent heat flux is primarily due to canopy transpiration, with a smaller contribution from direct soil evaporation (~20%) and a very small contribution from direct canopy evaporation. This is consistent with the statement above that transpiration is the most efficient mechanism for water loss from vegetated soil.

In addition to the time series, vertical profiles of model-derived quantities were plotted with co-located observations when available. Profiles of potential temperature, temperature, mixing ratio, and relative humidity were plotted. Shown in Fig 4 are profiles of potential temperature for the LSM (Fig 4a) and then control (Fig. 4 b). The LSM 17 h forecast is ~1 C too cool and the boundary layer depth is 100-200 m greater than observed. The control is 2-3 C too cool with the boundary layer depth approximately correct. In order to view the diurnal boundary layer evolution, profiles of potential temperature from the model are plotted in Fig 5 at 6 h intervals from 1900 LT 6 June to 1900 LT 7 June 2002. Several features are of interest. The initial profiles are the same and the 0100 profiles are similar. 0700 profile, however, shows a 13 C increase in potential temperature over the lowest ~100 m for the LSM and a 4.5 increase for the control. Given the strong stability in the LSM, it might be anticipated that the 1300 LT profiles would be cooler and the boundary layer shallower. In fact, the mixed layer is twice as deep (800 m vs 1600 m) and 3 C warmer in the LSM. At 1900 LT 7 June, the LSM has a mixed layer depth of 2 km (1600 m in the control) and is 3 C warmer.

4. CONCLUSIONS

Only preliminary conclusions are available. The biases in the LSM model seem to be similar to, but less than, those in the control. These include a negative bias in the wind speed, mixing ratio, and ground surface heat flux and a positive bias in the stress,

Acknowledgements: This research was supported by the Office of Naval Research Program Element 0601153N.

In the simulations reported herein, the soil and vegetative properties were obtained from a global agricultural meteorology (AGRMET) database with 45 km horizontal resolution. Thus, the surface characteristics on the 4 km inner nest were rather poorly resolved. We plan to re-run the simulations with a nearly completed 4 km resolution AGRMET data base obtained from running the soil model off-line for 18 months prior to the June 2002 period of interest. We will present these results at the conference.

REFERENCES

- Chang, J.-T., and P. J. Wetzel, 1991: Effects of spatial variations of soil moisture and vegetation on the evolution of a prestorm environment: A case study. *Mon. Wea. Rev.*, **119**, 1368-1390.
- Chen, F., K. Mitchell, J. Schaake, Y. Xue, H. Pan, V. Koren, Y. Duan, M. Ek, and A. Betts, 1996: Modeling of land-surface evaporation by four schemes and comparison with FIFE observations. *J. Geophys. Res.*, **101**, 7251-7268.
- Mahrt, L., and M. Ek, 1984: The influence of atmospheric stability on potential evaporation. *J. Climat. Appli. Meteorol.*, **23**, 222-234.
- Noilhan, J., and S. Planton, 1989: A simple parameterization of land surface processes for meteorological models. *Mon. Wea. Rev.*, **117**, 536-549.
- Pan, H-L., and L. Mahrt, 1987: Interaction between soil hydrology and boundary-layer development. *Bound. Layer Meteorol.*, **38**, 185-202.
- Pielke, R.A., 2001: Influence of the spatial distribution of vegetation and soils on the prediction of cumulus convective rainfall. *Rev. Geophys.*, **39**, 151-177.
- Weckwerth, T. M., and Coauthors, 2004: An overview of the International H₂O project (IHOP_2002) and some preliminary highlights. *Bull. Amer. Meteor. Soc.*, **85**, 253-277

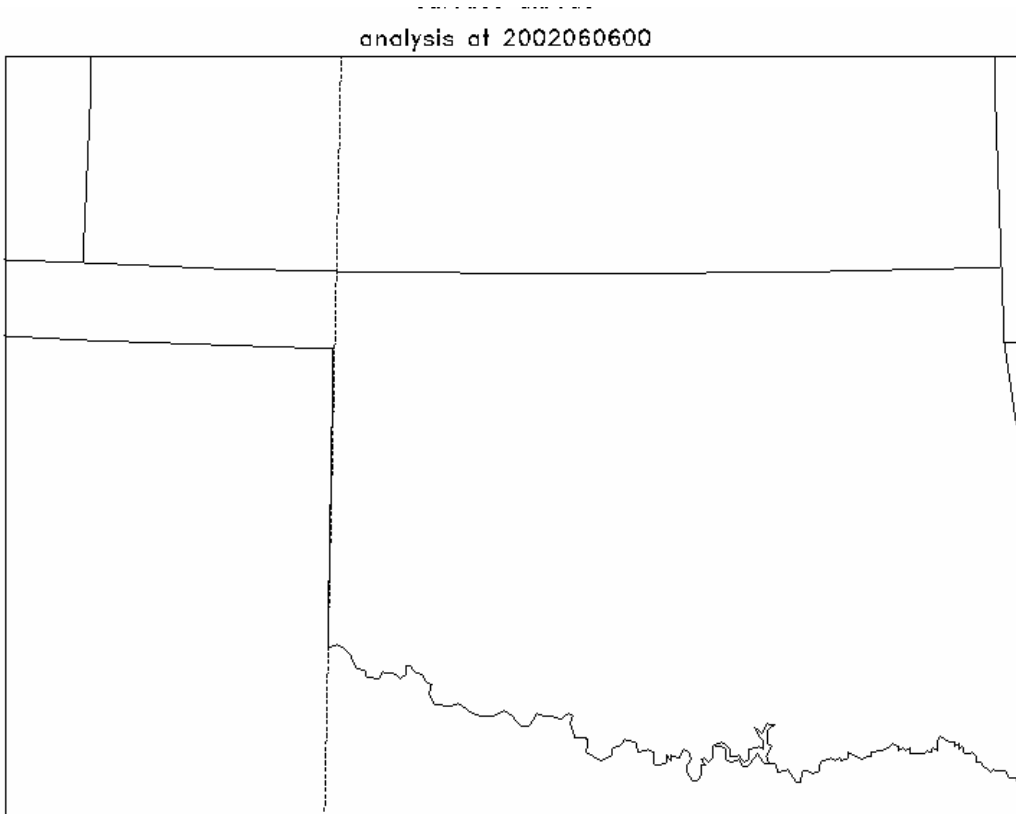


Figure 1. Nest 3 domain (4 km resolution) for IHOP-2002

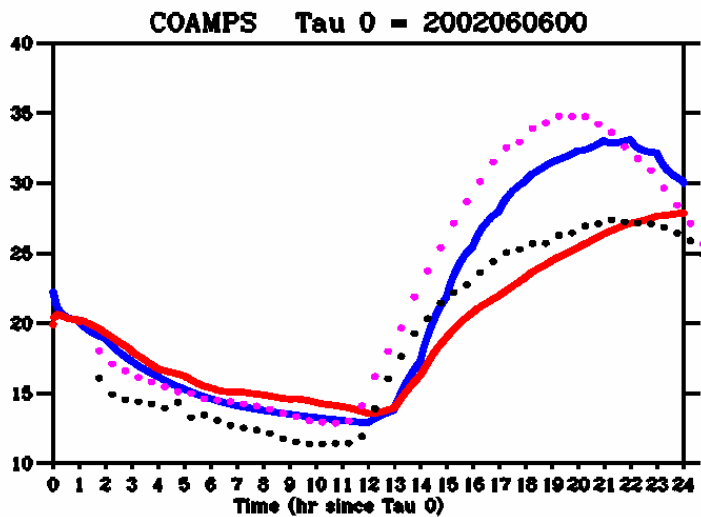
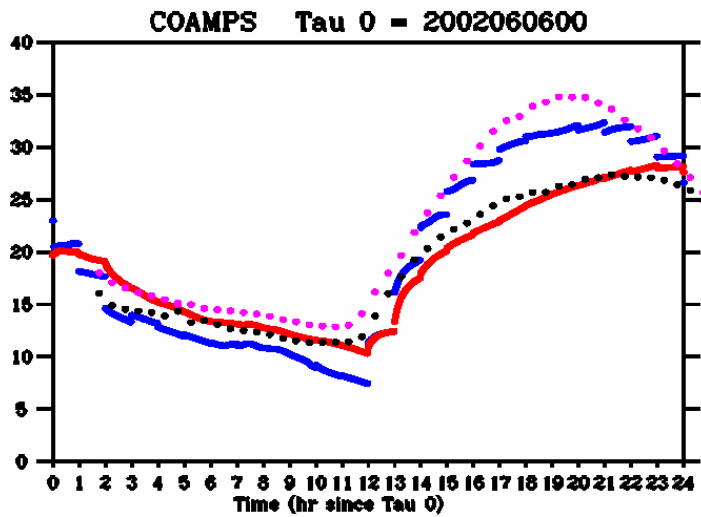


Figure 2. Time series of surface temperature and 2 m air temperature for a) the LSM and b) the control simulations. The solid blue line is the model surface temperature, the solid red line is the model 2 m air temperature, the dotted black line is the observed 2 m air temperature, and the dotted magenta line is the observed surface temperature. Observations are from station 4.

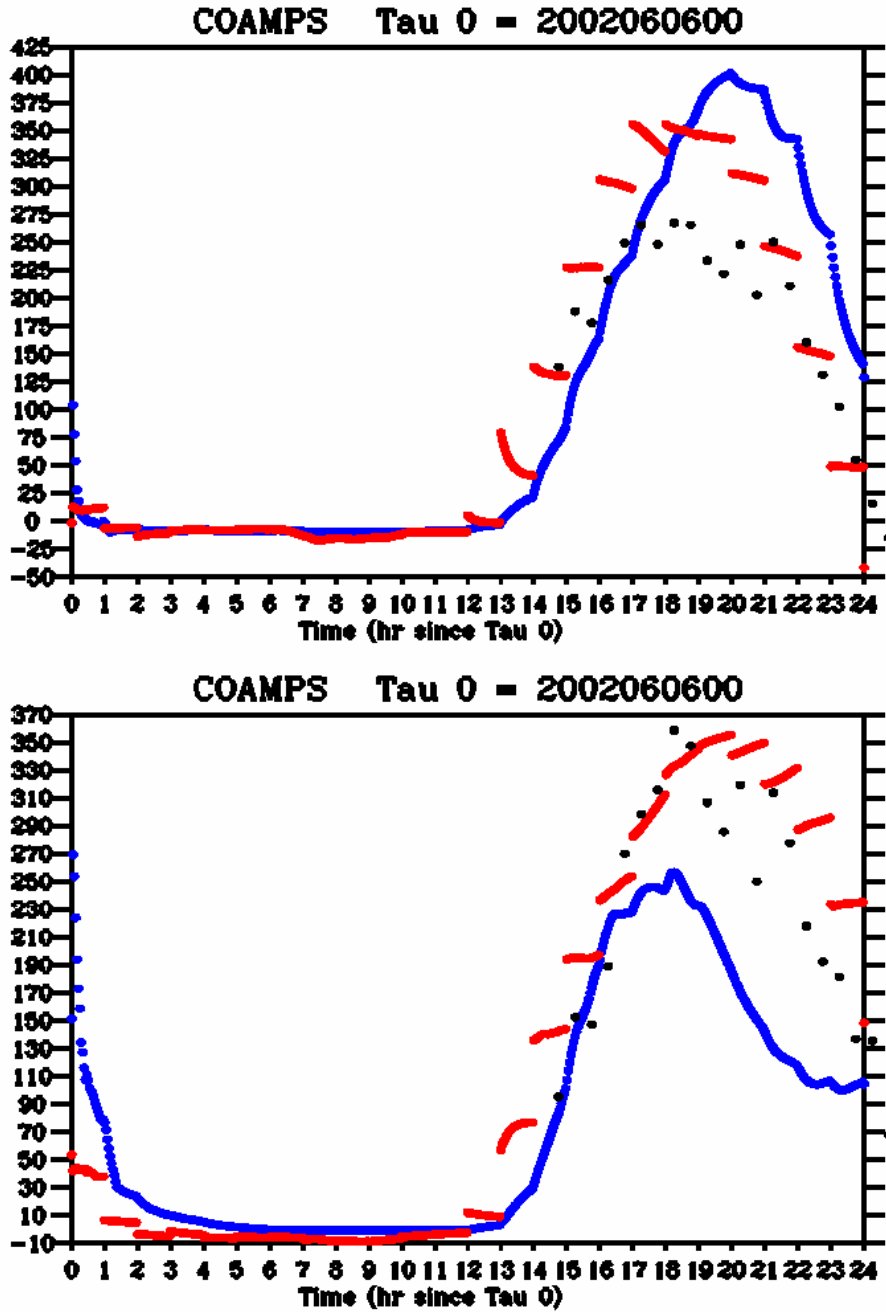


Figure 3. Time Series of a) sensible and b) latent heat flux ($W m^{-2}$). The dashed red line is from the LSM, the solid blue line is from the control, and the dotted black line is from the observation at station 4.

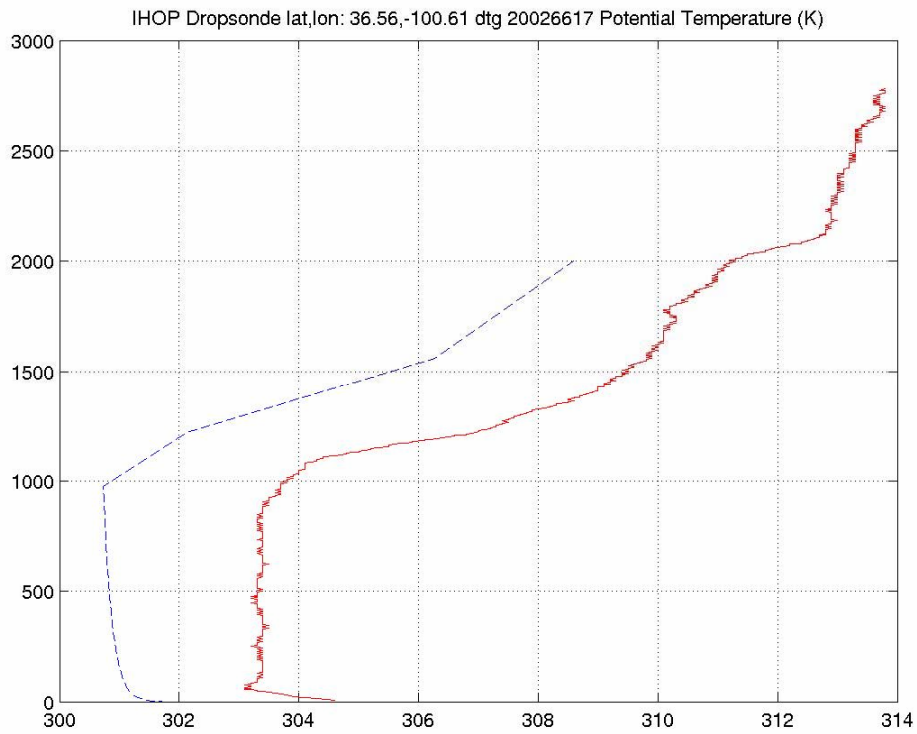
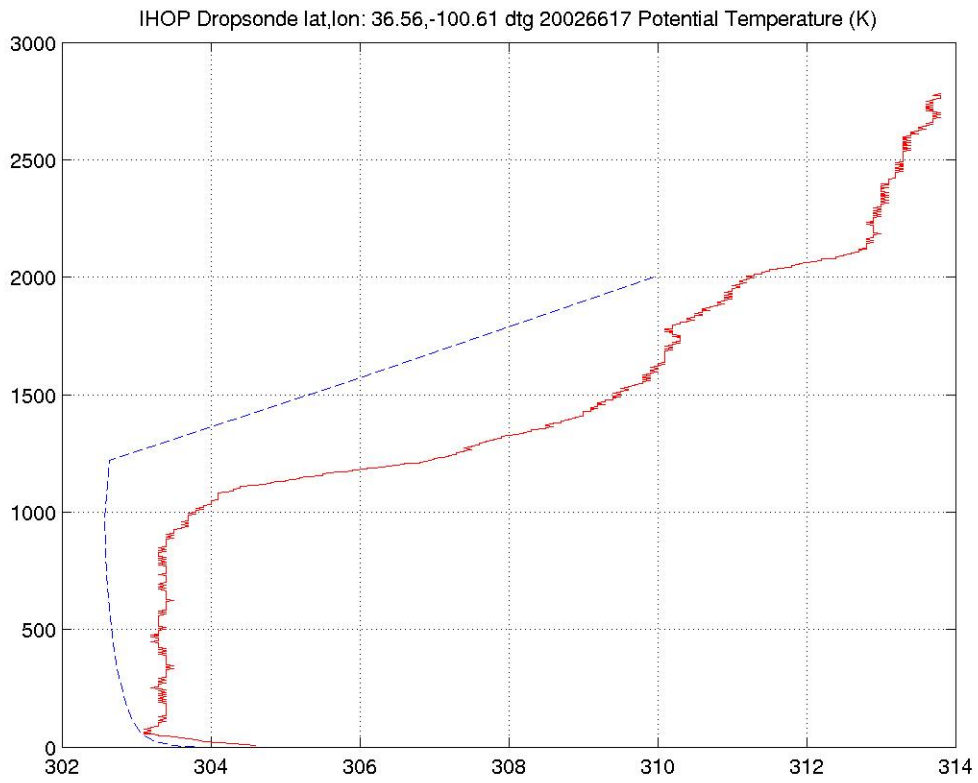


Figure 4. Profiles of observed (solid) and modeled potential temperature for a) LSM and b) control.

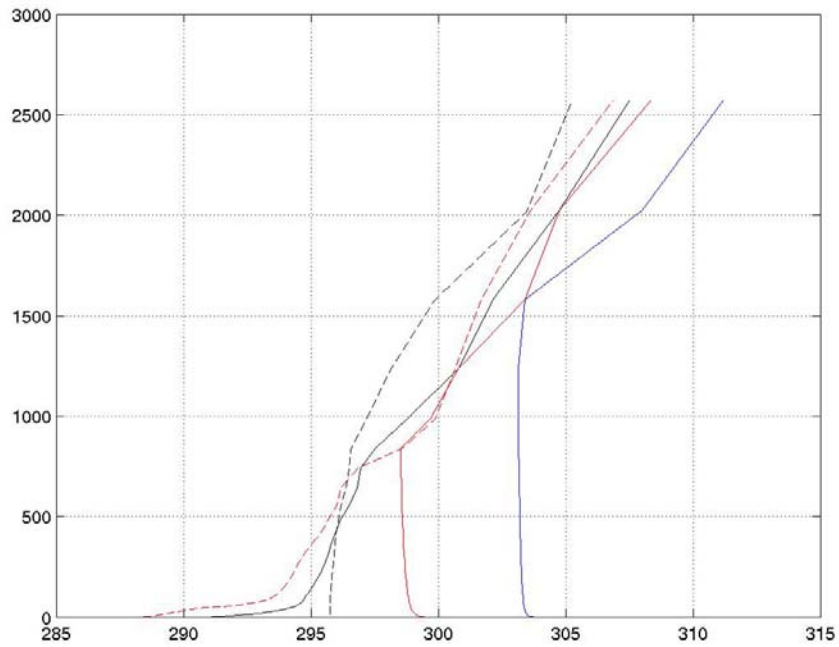
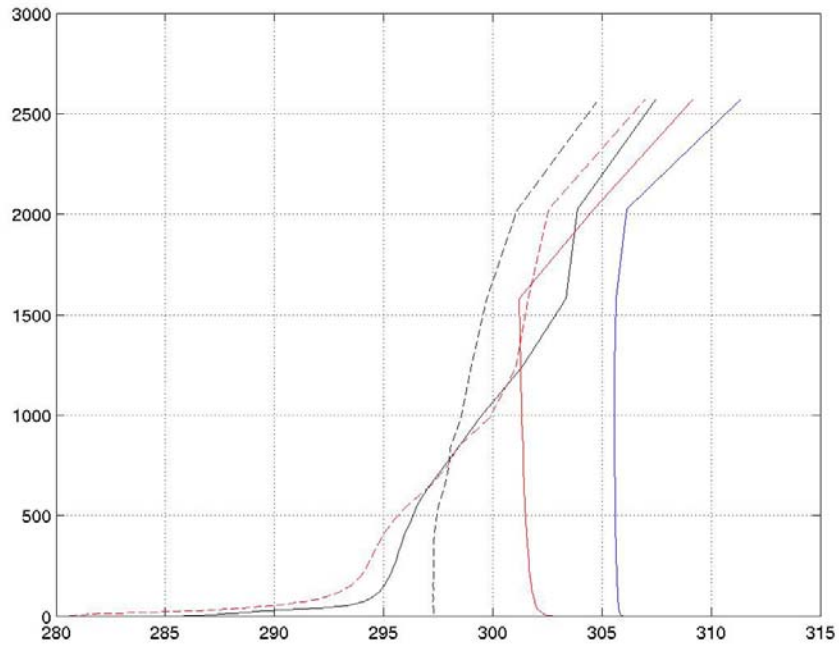


Figure 5. Profiles of potential temperature for a) LSM and b) control. The dashed black line is for 0000 UTC (1900 LT), the solid black line is for 0100 LT, the dashed red line is for 0700 LT, the red line is for 1300 LT, and the blue line is for 1900 LT 7 June 2002.

26
Table